United States Department of the Interior
Geological Survey

A Field Study of Large-scale Oscillation Ripples in a Very Coarse-grained, High-Energy Marine Environment

by
Donald W. Hirschaut
John R. Dingler

Open-File Report
82-733

A Field Study of Large-Scale Oscillation Ripples in a Very Coarse-Grained, High-Energy Marine Environment

Abstract

Monastery Beach, Carmel, California is a pocket beach that sits within 200 m of the head of Carmel Submarine Canyon. Coarse to very coarse sand covers both the beach and adjacent shelf; in the latter area incoming waves have shaped the sand into large oscillation ripples. The accessibility of this area and a variable wave climate produce a unique opportunity to study large-scale coarse-grained ripples in a high-energy environment. These ripples, which only occur in very coarse sand, form under the intense, wave-generated currents that exist during storm conditions. Once formed, these ripples do not significantly change under lower energy waves.

On three separate occasions scuba divers measured ripples and collected sand samples from ripple crests near fixed reference stakes along three transects. Ripple wavelength and grain size decreased with an increase in water depth. Sediment sorting was best closest to the surf zone and poorest at the rim of Carmel Canyon. Cobbles and gravel observed in ripple troughs represent lag deposits.

Carmel Canyon refracts waves approaching Monastery Beach such that wave energy is focused towards the northern and southern portions of the beach, leaving the central part of the beach lower in energy. This energy distribution causes spatial variations in the ripples and grain sizes with the shortest wavelengths and smallest grain sizes being in the central part of the shelf.

A Field Study of Large-scale Oscillation Ripples in a Very Coarse-grained, High-energy Marine Environment

INTRODUCTION

Several studies have been conducted on the small- to medium-scale ripples that often form in fine to medium sand subject to wave-generated currents. Conversely, there have been few field studies that focus upon the large-scale ripples that form in very coarse-grained sediments (Miller and Komar, 1978). The objective of this study is to fill this gap by providing new insights on the dynamics of coarse-grained sediments. This objective was reached by recording temporal and spacial changes in ripple characteristics and grain size at Monastery Beach, California. The study began in December, 1980 and ended in May, 1981.

Oscillation ripples have been defined as a systematic series of undulations, or waves, that form at the sediment-water interface under the influence of surface gravity waves (Inman, 1957). As a result, changes in the magnitude and direction of the wave energy produce changes in the ripples. The important factors that contribute to the observations presented in this study include: location of the study area, which influences exposure to wave energy; sediment supply; grain size; and local bathymetry.

Previous Work

Several investigators have examined Monastery Beach and the adjacent submarine canyon, Carmel Canyon, in differing degrees of detail. Wolf (1966) compared processes of erosion and sedimentation near the head of the canyon; he observed changes in ripple size that he attributed to depth and grain-size changes. Moritz (1968) described the general physiography of the canyon head, giving a probable history of events leading up to its present-day morphology. Griffin (1968) studied the heavy minerals at every Carmel Bay beach and determined mineral suite characteristics for each. Long (1973) conducted a limited field study of the oscillation ripples off Monastery Beach and suggested a possible genesis. He concluded that there is good correlation between ripple height or length and both grain-size and wave energy. However, his data was not quantitative enough to sufficiently establish this correlation. Hirschaut (1980) surveyed the central part of the study area. He documented, during one transect, changes in ripple and grain sizes with depth. Dingler (1981) examined the stability of Monastery Beach over a three-year period. He suggested that ripples act as a reservoir by trapping sand and slowly feeding it back onto the beach face during low energy conditions. He also found that the beach changes slowly in profile because offshore sand is tied up in the large oscillation ripples, and sand transport occurs at the rate of net ripple migration.

Location

Monastery Beach is located in the southeast corner of Carmel Bay, one kilometer south of the Carmel River mouth and one kilometer north of Point Lobos State Reserve (Figs. 1 and 2). Much of the littoral zone in this area is composed of very coarse to granular sand; however, the coastline adjacent to Monastery Beach consists of outcrops of the Santa Lucia granodiorite

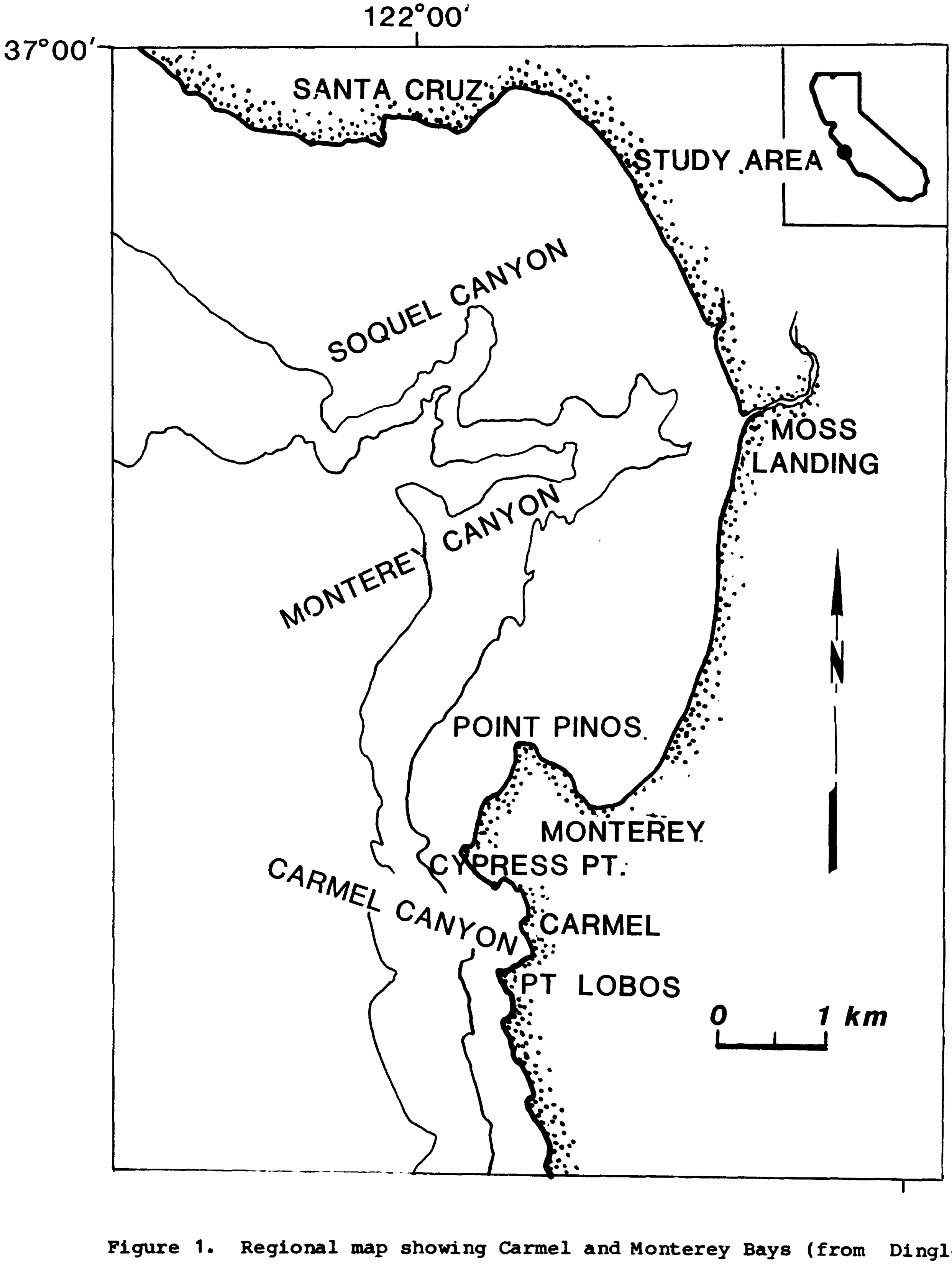

Figure 1. Regional map showing Carmel and Monterey Bays (from Dingler, J.R., 1981).

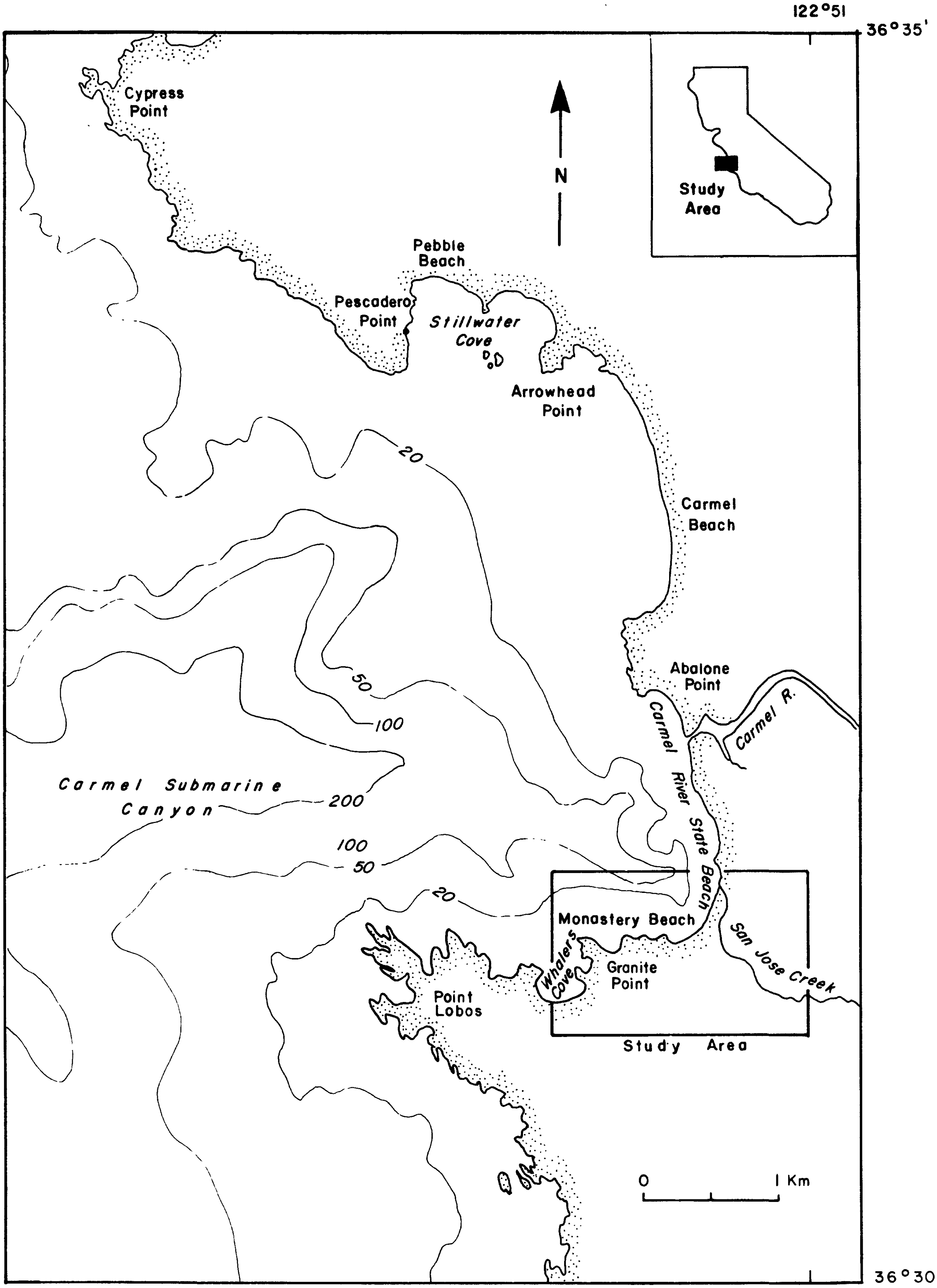

Figure 2. Detailed map of Carmel Bay showing location of study area and selected bathymetric contours of Carmel Submarine Canyon (from Dingler 1980).

(Wallin, 1968). These rocky headlands are highly resistant to erosion and, thus, create natural boundaries that restrict longshore transport from moving beach sand any appreciable distance (Griffin, 1969). As a result, Monastery Beach may be considered to be a large pocket beach (average length 600 meters), which has local sources of sediment (Shepard, 1973). These sources probably include the Santa Lucia granodiorite, the Carmelo Formation, the Carmel River, and San Jose Creek. The Carmelo Formation is a conglomeratic unit that crops out along the seacliff at the southern end of Monastery Beach (Fig. 3) and consists of cobbles set in a medium sand matrix (Wallin, 1968). Both the Carmel River, which enters Carmel Bay at the north end of Carmel River State Beach, and San Jose Creek, which enters at Monastery Beach (Fig. 2), are ephemeral in nature, flowing only during winter months (Moritz, 1968). During this study, San Jose Creek flowed for a period of at least three weeks. Regarding the importance of these sand sources, Wallin (1968) states, "The contribution to the sand budget by San Jose Creek is secondary." He also states that the Carmel River was a primary contributor of sand to the sand budget of the Monastery Beach area. This study did not attempt to quantify the various contributions of sediment to the area.

Carmel Canyon

Carmel Canyon heads within a few hundred meters of Monastery Beach. The canyon rim occurs in depths ranging from 12 to 15 m and is defined by a distinct break in slope (Fig. 4). The slope of the shelf between the canyon rim and toe of beach is a few degrees at most. At the shelf break the canyon steepens rapidly (Fig. 5) to 30 to 35 degrees (Dingler, 1981; Wallin, 1968; Moritz, 1968), which is the angle-of-repose for sand

Shelf Area

The nearshore portion of the study area is covered with large-scale, long-crested oscillation ripples. These ripples are the primary focus of this study. The ripples form in direct response to waves impinging upon the coast. The orientation of Monastery Beach restricts wave approach to a window between 270°-322° N (Dingler, 1981). Any waves from directions outside of this window either will not reach Monastery Beach or will refract and to some degree dissipate before reaching Monastery Beach. Wave statistics for this area show that 90% of all deep water wave energy comes from the northwest quadrant (National Marine Consultants, 1960). Thus, high-energy, northwesterly storm waves approach Monastery Beach with little wave refraction occurring, until they cross the canyon head. The combination of large wave energy and a very coarse beach creates a steep beach face (10°-12°) with a berm crest that is 5 m above mean low water level (Wallin, 1968). The tidal pattern is classified as mixed, containing mainly semi-diurnal components, with a range of 1.6 m between mean higher high water, and mean lower low water (Dingler, 1981).

METHODS

Reference Grid

All observations were made by scuba divers, who directly measured the ripples. A total of 20 scuba dives were made on 7 different days during the

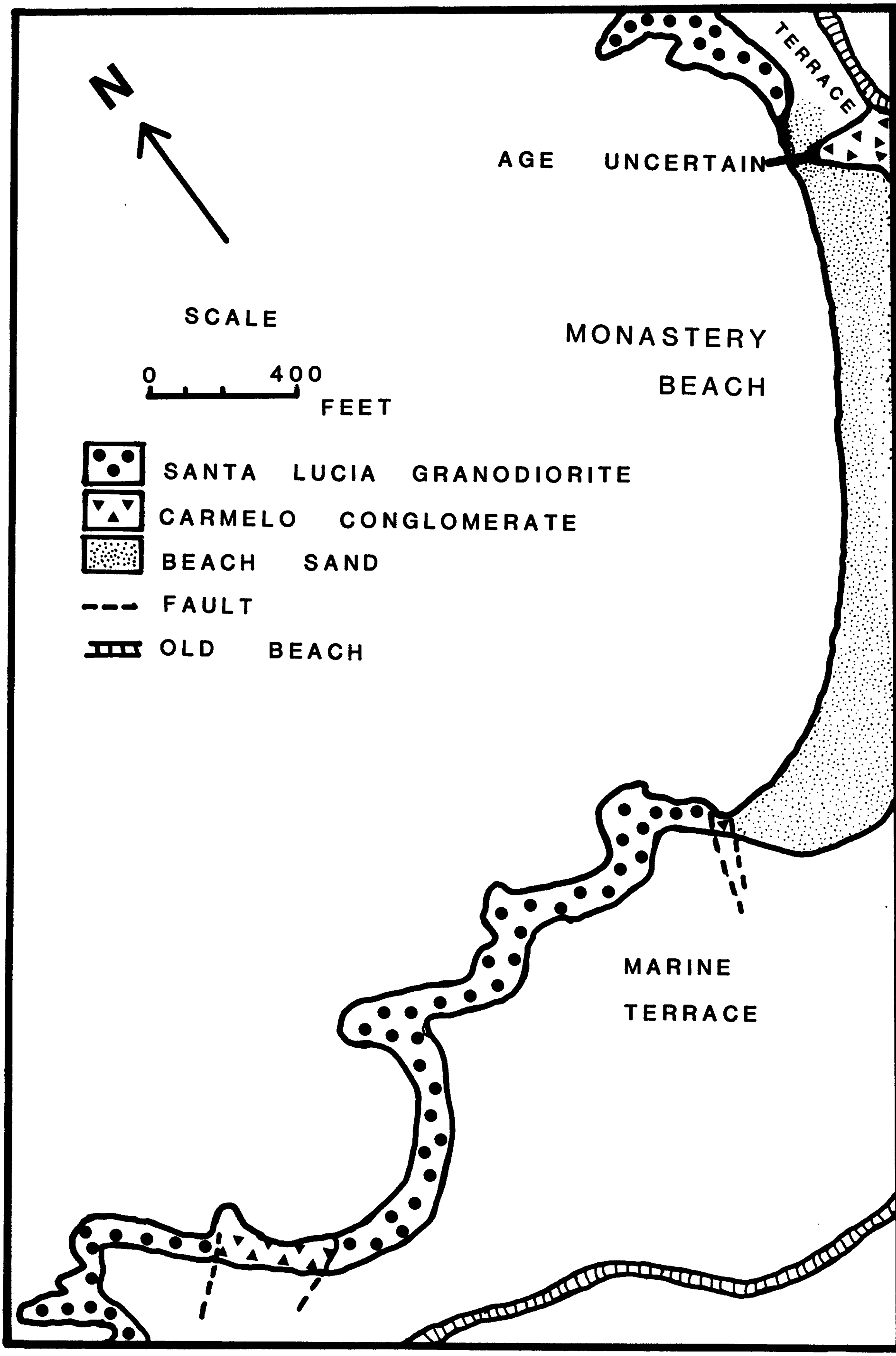

Figure 3. Geologic map of local shoreline. Note granitic headlands exposed at both ends of Monastery Beach. Also note small sea cliff exposure of conglomeratic unit at south end of beach (from Wallin, S.R., 1968).

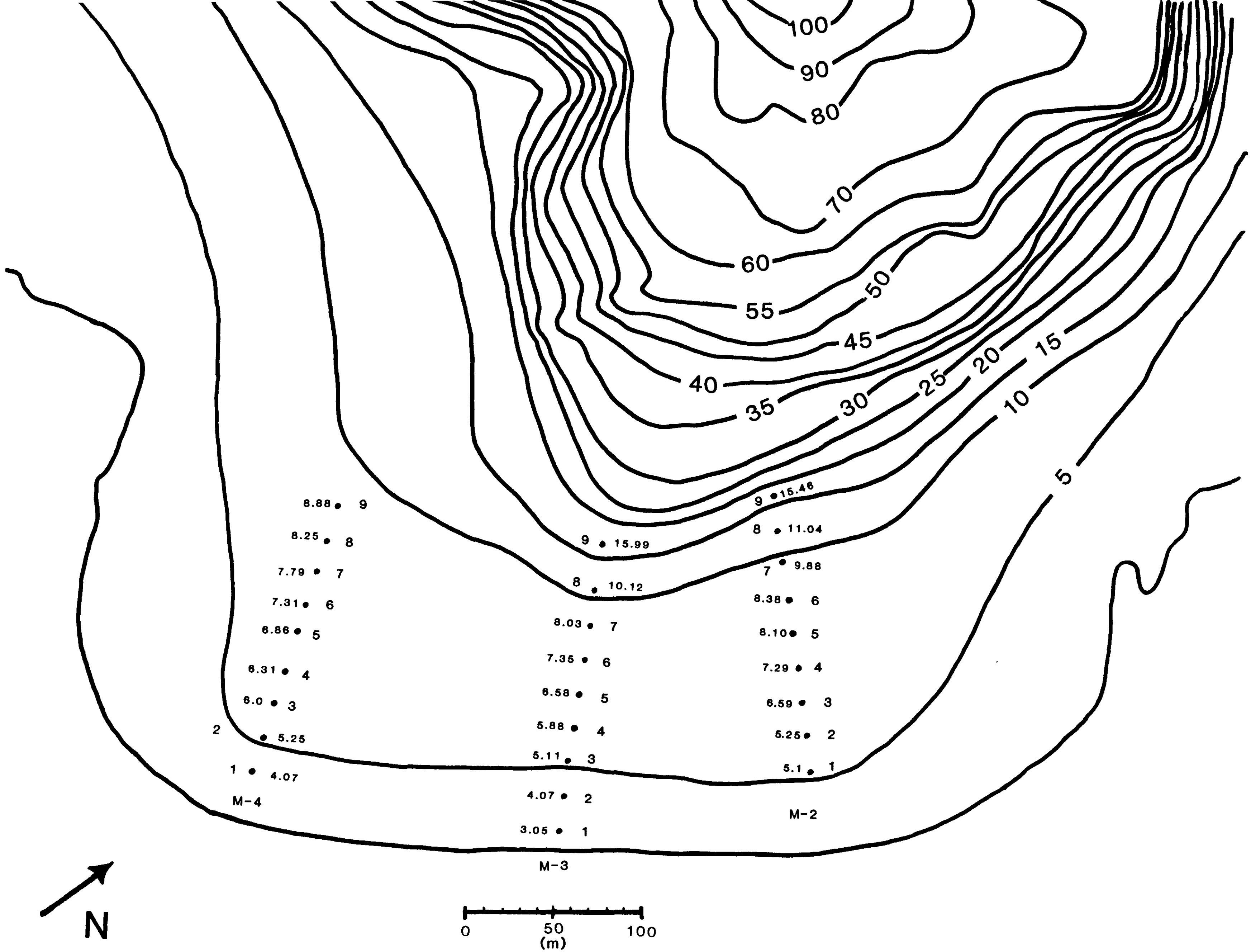

Figure 4. Bathymetry in the area off Monastery Beach, numbered dots represent reference stake locations transects along M-2, M-3, and M-4. The mean depth of each stake is adjusted to mean sea level. Note position of Carmel Canyon; it heads within 200 m of the beach.

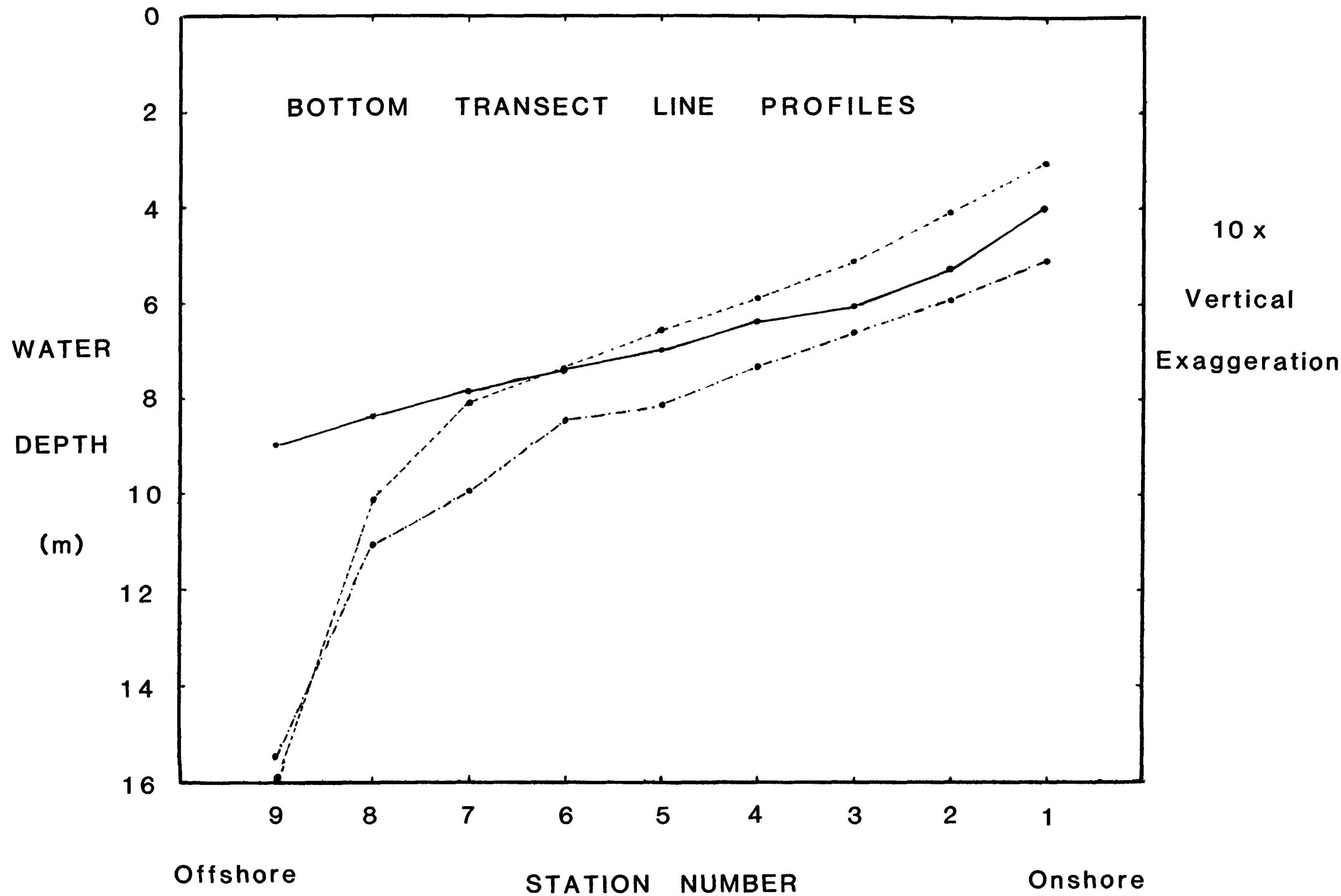

Figure 5. Mean depths of reference stakes. The bottom slope between stations 1 and 6 is a few degrees at most. A rapid increase in slope to 30-35° occurs at station 8, lines M-2 and M-3, marking the rim of Carmel Submarine Canyon. Refer to Fig. 4 for station locations in plan.

course of this study. During the first 6 dives a grid of reference stakes was laid out. The grid consisted of 9 stakes on each of 3 shore-normal transects. On each line 2-m long steel pipes were driven approximately 1 m into the sediment at 20-m intervals (Fig. 4). To insure that the stakes lay along a straight line, nylon parachute cord was run from a known onshore position to a known offshore position. A 20-m length of nylon line provided a means of obtaining equal spacing between the stations. Reoccupation of each station was greatly facilitated by the exact initial positioning of each stake. This became especially important during times of poor underwater visibility.

The northernmost transect line was designated M-2, the central M-3, and the southernmost M-4, to correlate with the beach profile lines established by Dingler (1981). Along each line the stakes were numbered 1 through 9 from onshore to the offshore. Figure 4 shows the location and mean depth of the stakes.

DATA COLLECTION

Divers collected three sets of data; however, the first, taken on March 4, 1981, was incomplete due to large wave conditions. The second, taken on March 31, 1981, and the third, taken on May 17, 1981, were complete data sets. Subsequently, five dives were made to measure the precise depth of each station, and to tie-in each transect line to a land reference marker. An infrared surveying station with an accuracy of about ± 1 m was used for this purpose. The technique involved positioning a float that held a prism over selected stakes and measuring distance and angle from the surveying station to the prism.

Each transect line was completely sampled during one dive with the data being recorded onto waterproof paper. The divers took a ripple-crest sediment sample and measured the following paramaters at each reference station: depth, stake height, ripple wavelength, ripple height, ripple symmetry, and ripple orientation (Figs. 6 and 7).

A specially designed T square permitted rapid and accurate measurement of the large-scale ripples commonly found at Monastery Beach (Fig. 6). Five consecutive ripples were measured at each station to obtain a statistical average of each parameter (Miller and Komar, 1978). One diver oriented the T-square in an onshore direction; the other diver then recorded the length, height, symmetry, and crest bearing.

Each sand sample was collected in a small cloth sample bag (Fig. 8). The samples were washed, dried, and sieved at quarter phi intervals using standard laboratory grain-size analysis procedures (Folk, 1974). The cumulative percents by weight were calculated, and cumulative curves drawn on semi-log paper (Appendix 1). The median, mean, standard deviation, skewness, and kurtosis descriptive measures were calculated for each sample using the technique of Inman (1957).

Upon arriving at a stake, the water depth was measured using a standard, oil-filled diver's depth gage, which has an accuracy of ±1 m at best. Exact depths were later recorded using a precision digital depth gage designed to be accurate to 0.01 m (Fig. 9). Times were recorded for each series of depth measurements so that the depths could be corrected to mean sea level using the National Ocean Survey Tide Tables (1981).

The amount of erosion or deposition at each reference stake was obtained

Figure 6.

Diver setting up T-square at reference stake to measure a coarse grained osclation ripple.

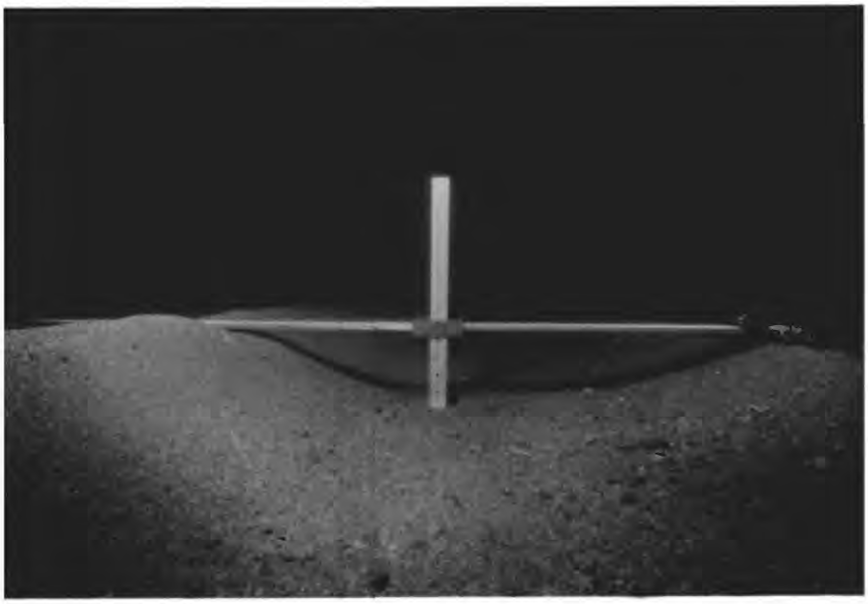

Figure 7.

Measuring ripple height with the T-square.

Figure 8.

Diver collecting ripple-crest sand sample.

Figure 9.

Divers taking precision depth measurements at reference stations. Note u/w paper for recording measures.

Figure 10.

Diver taking height with T-square at a reference stake (Note compass and depth gauge).

by measuring the stake heights during each sampling period (Fig. 10). Initially we did not account for ripple migration, which can change the sand-to-stake-top distance irrespective of whether erosion or deposition occurred. Because the stake heights were not standardized until the third set of measurements, comparisons with the initial stake or second stake height data would not be reliable. To get some indication of net sediment movement, we measured the stakes a fourth time on July 15, 1981. This data can be reliably compared with that collected on May 17, 1981, because both sets of measurements were taken from the top of the nearest ripple crest to the top of the stake.

RESULTS AND DISCUSSION

Mean Grain Size

In general, the mean grain size increased with a decrease in water depth. This trend conforms well with the trend predicted by wave theory (Miller and Zeigler, 1964). However, grain-size values from two of the shallowest stations oppose this trend. This tendency occurs at depths between 3 and 6 m, on lines M-3 and M-4 (Fig. 11). The observed decrease in the grain-size trend could reflect variations of wave energy or be the result of patches of finer sand unevenly distributed in the offshore. When examining Figure 11, it is readily apparent that the central portion of the beach (line M-3) is composed of finer-grained sand than either the northern (M-2) or southern (M-4) areas. The submarine topography of the area (Figs. 4 and 5) may focus wave energy to the flanks of the canyon (Fig. 12), as well as reflect some of the energy back towards incoming swells. This would have the effect of minimizing energy in the central portion of the beach, and concentrating it on the margins (Shepard, 1973; Komar, 1976, p. 112).

The type and amount of material available to Monastery Beach is very important in determining the textural characteristics of the sediments in this area. The grain size distribution can be interpreted to occur because of the proximity to the source areas that provide material to the beach. If local erosion of the Santa Lucia granodiorite at the ends of the beach is significant, then we would expect to find the coarsest material at the northern and southern ends of the beach.

Ripple Wavelength

Plotting average ripple wavelengths against depth produces an inverse relationship. Because the ripple wavelength decreases, as depth increases, these are orbital ripples (Clifton, 1976). The exception to this trend occurs at the most onshore stations, which are in water less than 6 m deep. Upon examining Figure 13, it can be seen that on some of the survey days, the ripples at station 1 are shorter than those at station 2. This tendency is attributed to an increase in the near-bottom wave orbital diameter beyond the value required to produce a maximum ripple wavelength (Inman, 1957). As a wave approaches the shore, orbital diameters increase in size with decreasing water depth. However, in the shallowest water the maximum ripple size is attained, and an increase in orbital diameter actually decreases the ripple wavelength, forming what Clifton (1976) calls suborbital ripples (Fig. 14).

When comparing ripple wavelengths along the transect lines against one another, a major division in sizes is evident. For a given depth, wavelengths

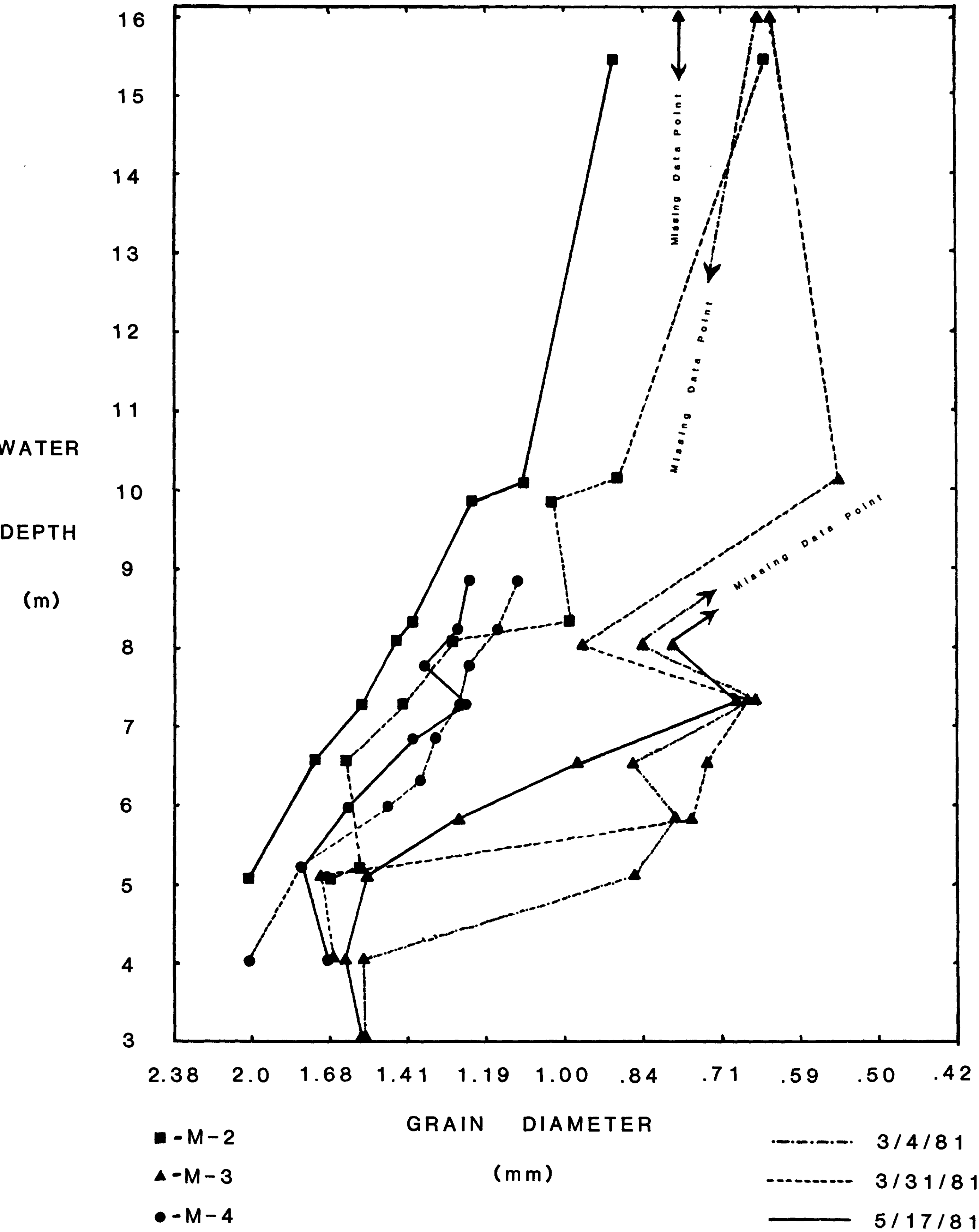

Figure 11. Mean grain size plotted against water depth. Note trend of grain size to increase with a decrease in water depth. Also note in shallow water between 3 and 6 m that this trend is sometimes reversed. Transect line M-3 is composed of finer grain sands overall. (Broken lines with arrow denote a missing data point at reference location M-3-8).

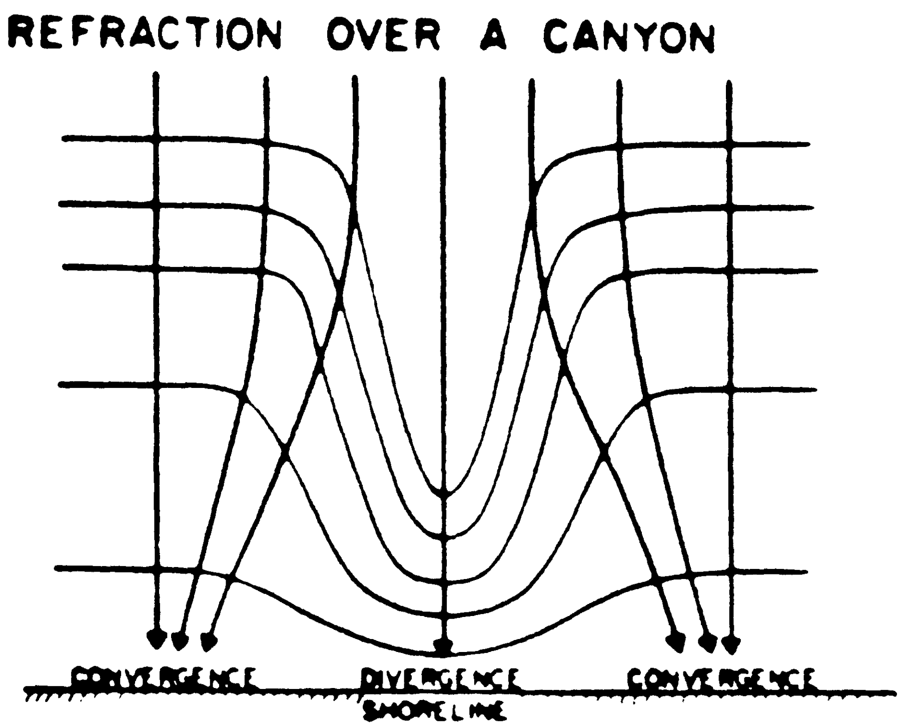

Figure 12. Wave refraction over a submarine canyon. Note how wave energy is concentrated at the flanks of the canyon and dissipated at the head (from Komar, 1976, p. 112).

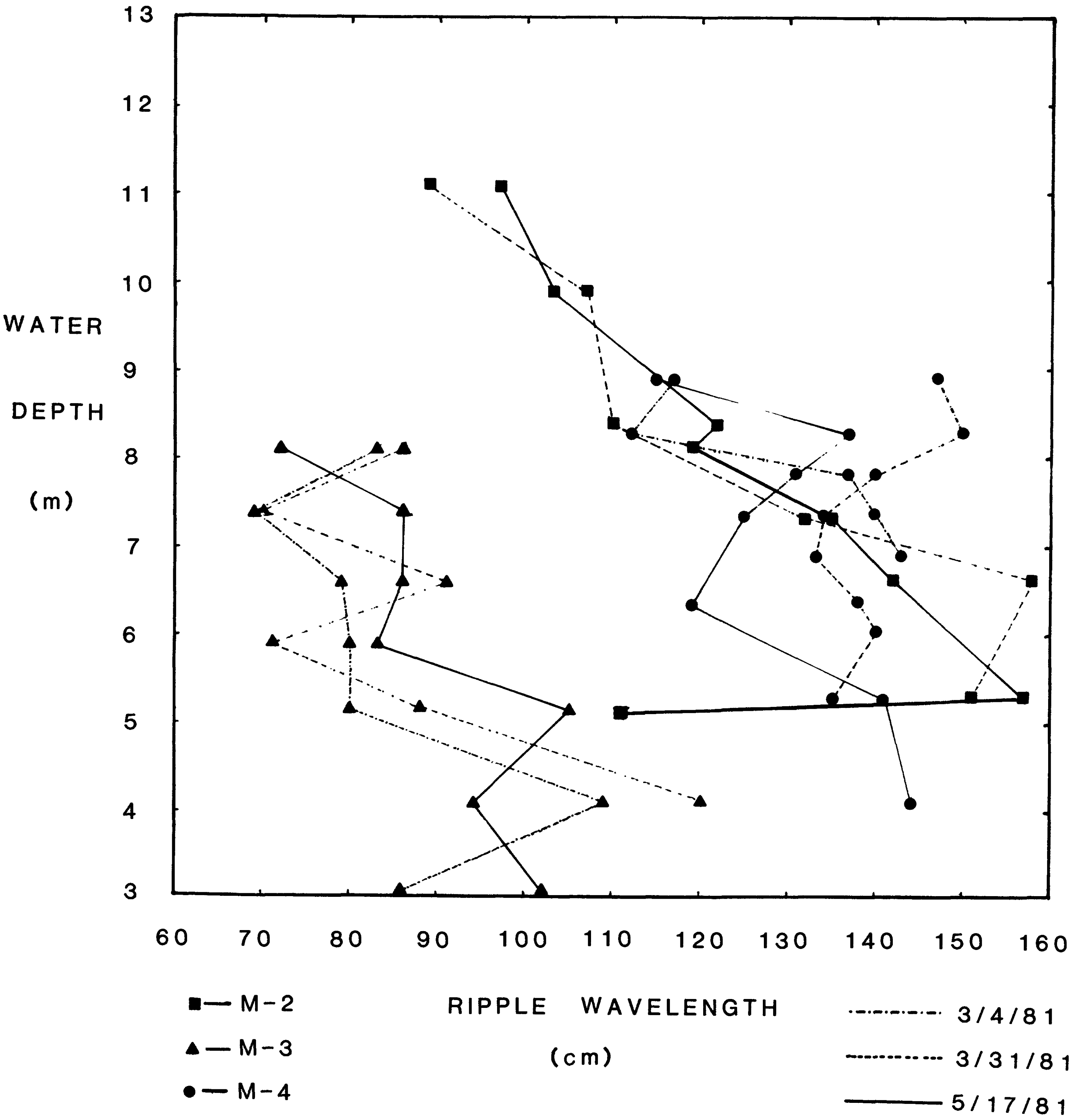

Figure 13. Average ripple wavelength versus water depth. Note inverse trend- as water depth increases ripple wavelength decreases. Transect line M-3 has much shorter average wavelengths than either M-2 or M-4. In shallow water at depths between 3 and 6 m the wave length often decreases in length, opposing the general trend.

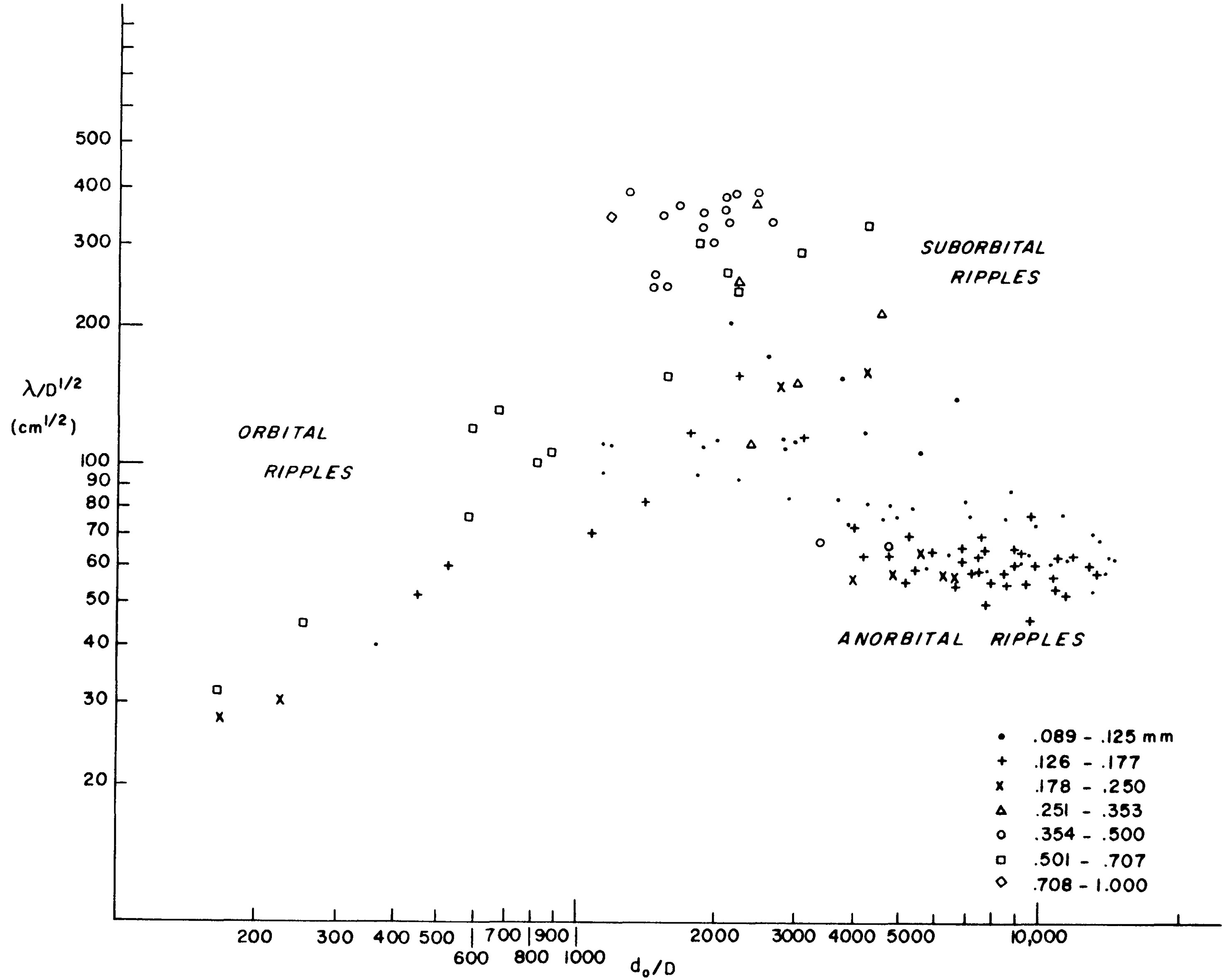

Figure 14. Relation between ratio of ripple wavelength to square root of grain diameter ($\lambda/D^{1/2}$) and ratio of orbital diameter to grain diameter (d_o/D) for oscillation ripples. The data from this study plots mostly as orbital ripples. However, several reversals in the grain size and wavelength do occur when d_o values become very large in shallow water. (From Clifton, 1976).

along M-3 are shorter than along either M-2 or M-4. The major reason for the smaller wavelengths of transect M-3 relative to those of the other lines is the grain-size difference previously described. Grain size has been shown to be the major factor affectng ripple wavelength (Dingler and Inman, 1976). During this study the average ripple wavelength at any given reference location did not change significantly. Thus the ripples are fairly stable over time, and once formed do not change easily. When comparing the average ripple wavelengths to the mean grain diameter at each reference location, a direct correlation is observed (Fig. 15). Scatter occurs because of grain sizes larger than 1 mm occur in shallow water on line M-3 and in deeper water on lines M-2 and M-4. Thus, the effect of orbital diameter is superimposed on the grain-size effect.

Ripple Symmetry

The ratio of the horizontal distance from a ripple crest to the first onshore trough (β) to wavelength (λ) is used as a measure of ripple symmetry (Fig. 16). Symmetrical ripples have β/λ ratios of 0.5; however, because of the margin for error inherent in measuring β, ripples with ratios between .45 and .55 are considered to be essentially symmetrical (Allen, 1968). Values of less than .45, or greater than .55, indicate that a ripple is asymmetrical. When the value is less than .45, the ripple's steep face points in the direction of wave propagation, while the opposite holds true for values greater than .55 (Inman, 1957).

For our data, 98 percent of the β/λ values are less than .55, 32 percent of all values are between .45 and .55, and 66 percent of all values are less than .45 (Fig. 17). Assuming that ripple asymmetry is an indicator of ripple migration (Allen, 1968), then the ripples are slowly moving onshore. However, the slight amount of asymmetry present may exist with no net ripple migration ever occurring. A conclusion of a field study conducted by Cook and Gorsline (1972) was that ripples may remain in the same position even though sediment and water are differentially transported.

Sand Deposition

A comparison of the stake height data of transects M-2 and M-4 on 5/17/81 and 7/15/81 respectively (Table 1) suggests that sand deposition occurred at most of the reference stations. The average deposition along transect line M-2 is 2.2 cm with the greatest change of 26 cm occurring at station 8, located at the canyon rim. The average net depositon of transesct line M-4 is 6.7 cm, with the greatest change of 15 and 18 cm occurring at stations 1 and 4. No reliable stake height data was obtained for transect line M-3.

Because of insufficient data, it is difficult to correlate the differences in stake heights with a net sediment movement. However, because the ripples did not change in size significantly between the two measurements, the differences appear to be real. Other studies have shown the largest changes in sand volume occur in depths of less than 10 m (Cook and Gorsline, 1972); however, in this case the proximity of the canyon head may produce a different pattern. Initial results from an ongoing field experiment at the canyon head near the offshore most stations of line M-2 between March, 1981 to June, 1981 show an average depositon of 10 to 20 cm just below the canyon rim.

This stake height evidence, along with other visual underwater

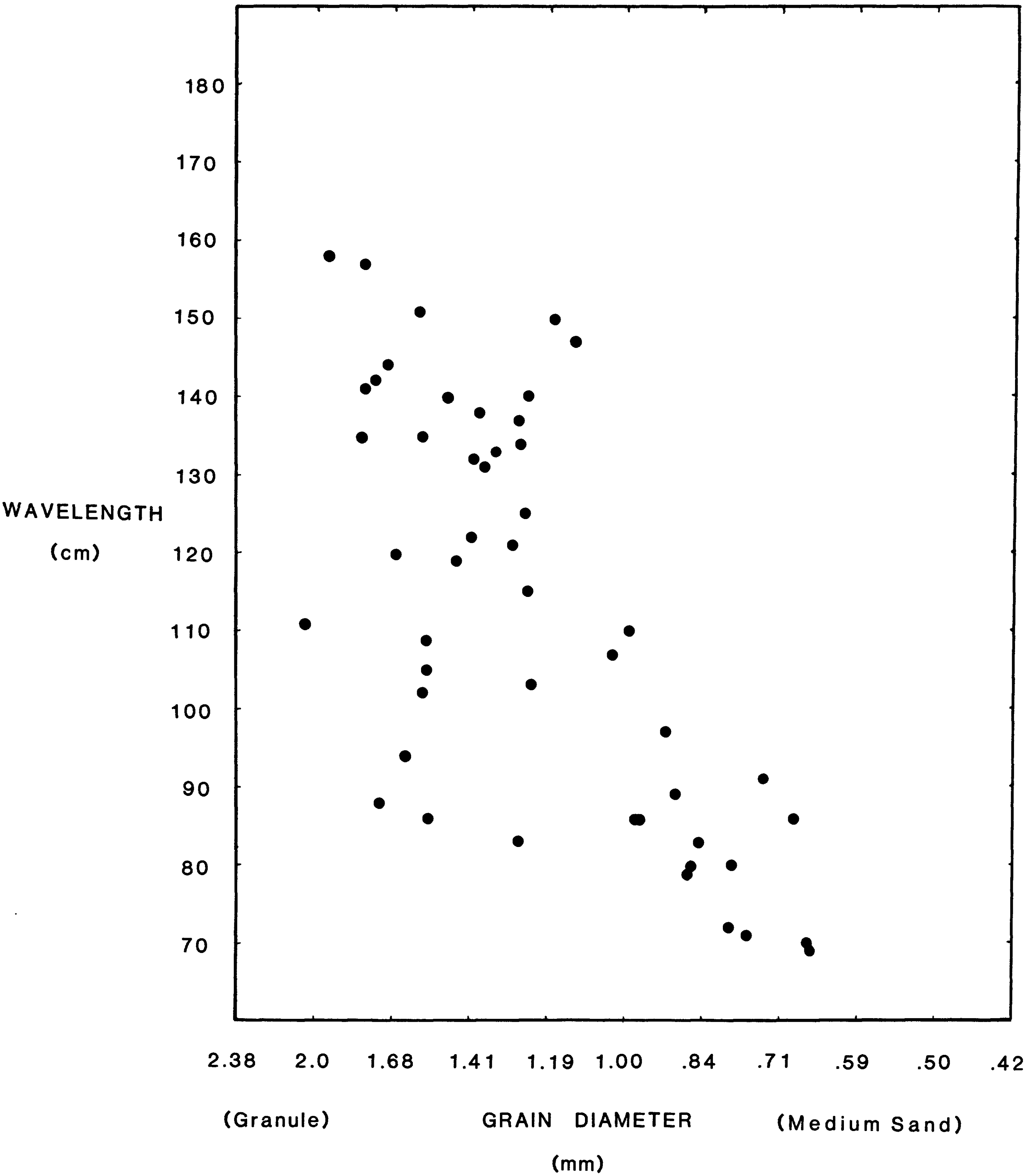

Figure 15. Plot of mean grain diameter versus ripple wavelength. Ripple wavelengths tend to increase as the mean grain diameter increases, although there is a fair amount scatter, especially for the largest grain sizes.

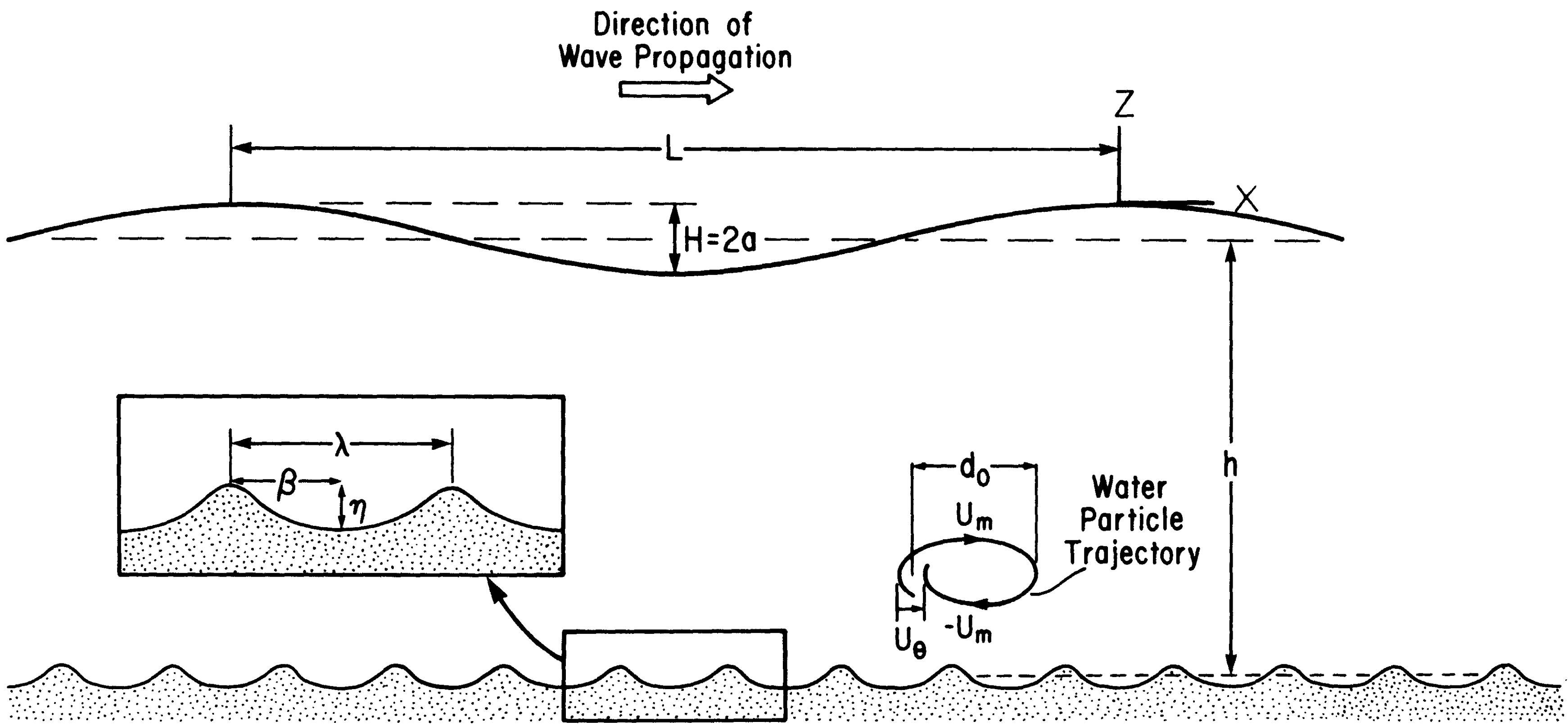

Figure 16. Definition sketch for wave and ripple parameters used in this study. The measure of symmetry used in this study is: (β/λ) symetrical ripples have a value of .5. From Dingler and Inman (1976).

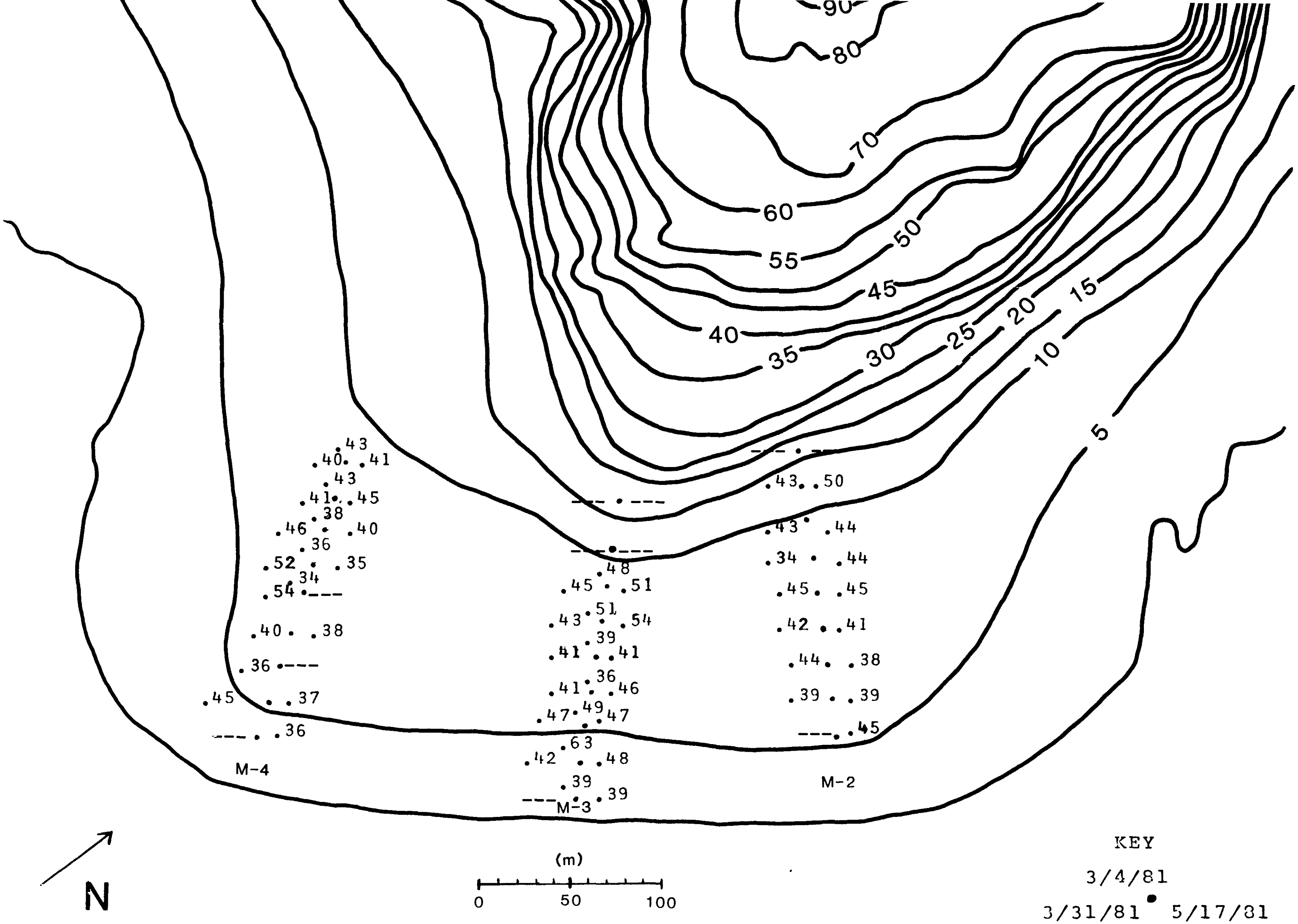

Figure 17. Average ripple symmetry values. A value of .5 results in a perfectly symmetrical ripple. 66 percent of all values are less than .45 indicating the steep (lee) face of the ripples is pointing in the direction of wave propagation. The majority of ripples thus exhibit a net onshore asymmetry.

observations, suggests that sand movement commonly occurs around the head of Carmel Canyon. At present it is believed that sand migrates seaward over the shelf-break and cascades downward into the canyon. This process is thought to be continuous and as such is slowly removing sand from the nearshore system in spite of the fact that many ripples have slight onshore asymmetrics.

Sediment Sorting

As part of the textural analysis of each sample, the phi standard deviation was computed. The standard deviation is a measure of sorting; the smaller the value, the better the sorting (Folk, 1974). Sorting was best closest to shore where wave energy is highest. Sorting was very poor at the most seaward location of each line and exhibited a distinct bimodal grain-size distribution.

In comparing the sorting temporally, the following trends are evident. Sand along transect line M-3 became more poorly sorted between March 4 and March 31, but it became better sorted between March 31 and May 17. Sand along line M-2 also became better sorted between March 31 and May 17. Sand along line M-4 remained unchanged in sorting values throughout the sampling period.

The observed sorting trends are interpreted to result because of large changes of average wave energy arriving to the area (Figs. 18, 19, and 20) and because of the San Jose Creek run-off occurring at this time. Wave statistics for this coast show the greatest energies arriving between March 4 and March 31 (Coastal Data Information, 1981). Because of this energy flux, grain diameter would begin to establish a new equilibrium position in the nearshore (Miller and Zeigler, 1978). As a result, sorting would become poorer until a new grain-size equilibrium had been established. The introduction of sediment into the nearshore by San Jose Creek would also have the effect of decreasing sorting, especially along the central and northern transects where the creek mouth flows. This correlates well with the observed data trend (Table 2).

Ripple Orientation

Our inability to resolve crest orientations to better than a few degrees makes it difficult to make quantitative deductions on the observed variations in ripple orientation. Furthermore, sinuosity of the ripples, which was observed in places but was not systematically documented, would increase the scatter in the orientation data. Ripple orientations on any given sample day generally parallel each other along a transect line (Fig. 21). The observed changes in ripple orientation from one day to another, if significant, would result from changes in the direction of wave approach. Usually, oscillation ripples orient themselves so that the crests are parallel to the wave crests above them. Wave refraction in shallow water, which occurs whenever the waves cross bottom contours at an angle, should result in a systematic change in ripple orientation across the shelf. The fact that ripples in the study area are parallel along a transect line but not parallel between lines suggests that wave refraction occurs primarily along the canyon flanks and not over the relatively narrow shelf.

Visual Observations

In addition to the quantitative data collected, several visual

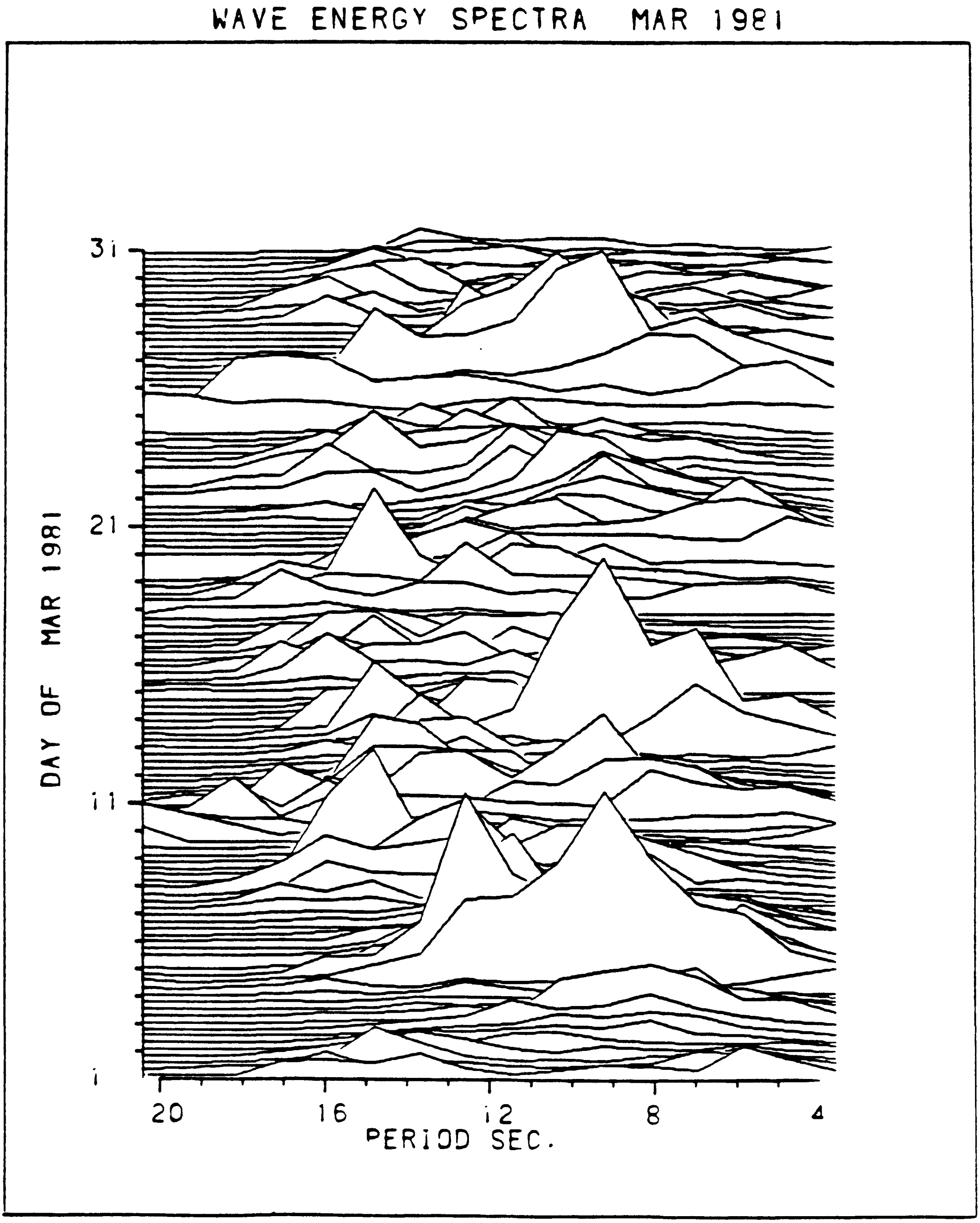

Figure 18. Deep water wave energy spectrum for month of March 1981. Notice periods of large wave energy immediately following collection of the first data set on 3/11/81 (from Coastal Data Information Program, 1981).

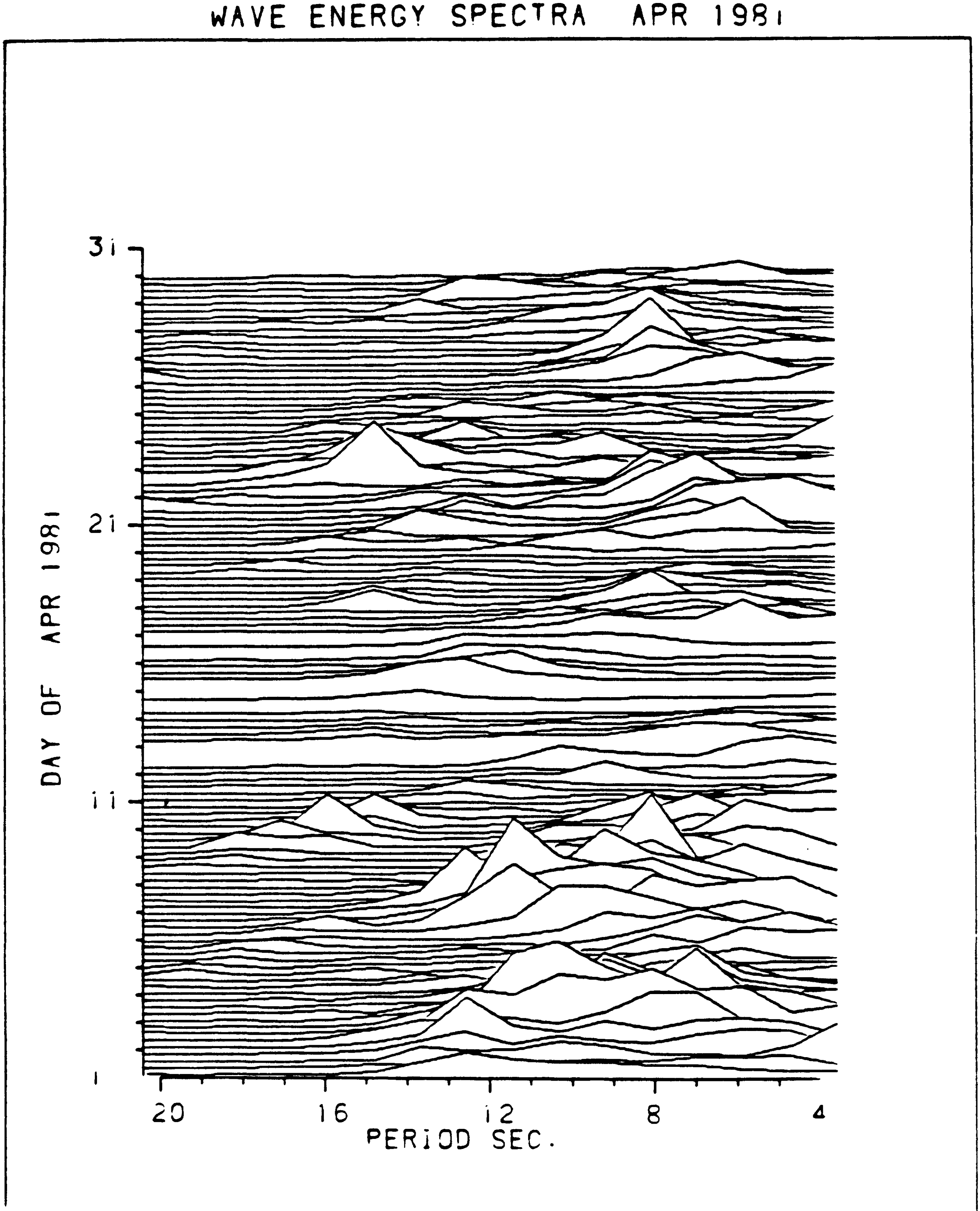

Figure 19. Deep water wave energy spectrum for month of April 1981. Notice intermediate wave energy to April 11, followed by low energy conditions (from Coastal Data Information Program, 1981).

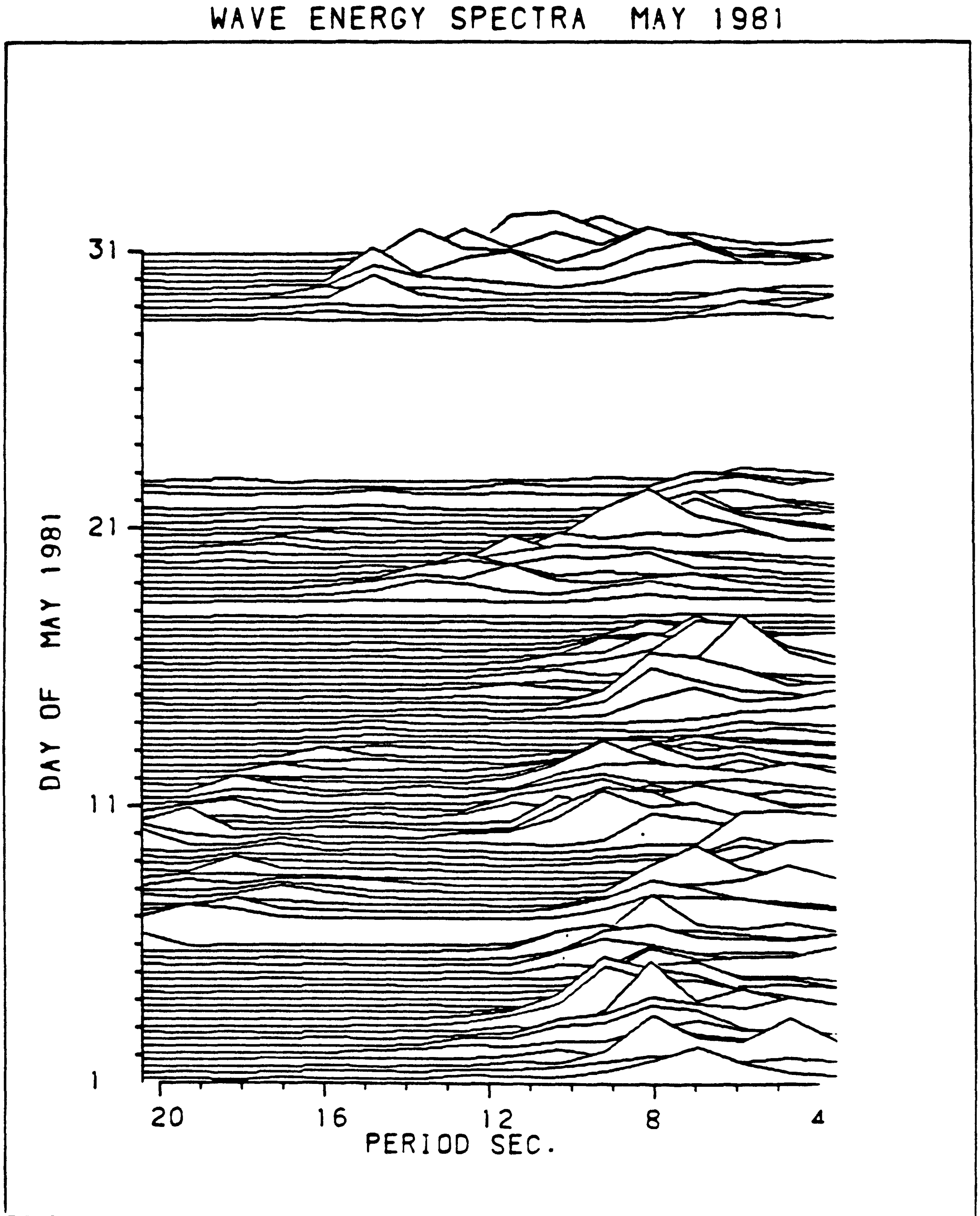

Figure 20. Deep water wave energy for month of May 1981. Notice occurrence of short period intermediate wave energy to the third data set collected 5/17/81 (from Coastal Data Information Program, 1981).

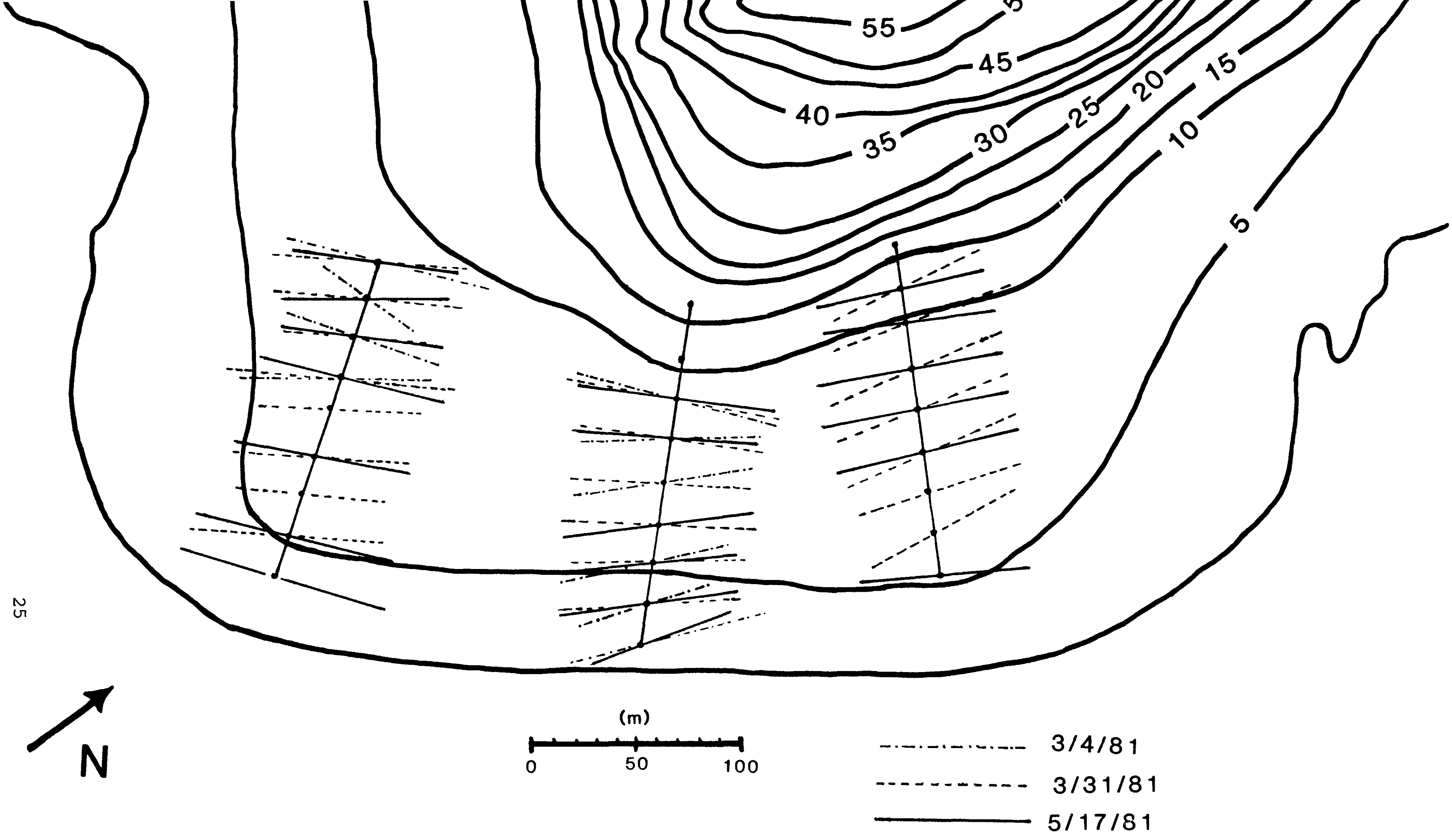

Figure 21. Ripple orientations for any sample day occur nearly parallel to one another and tend to follow bathymetric contours.

observations were made. San Jose Creek broke through the berm at the center of the beach in mid-March. By mid-April the creek bed had eroded the berm northward until the creek entered the ocean at the north end of the beach. The creek ceased flowing during the third week in April. Griffin (1969) observed a very similar situation during the winter of 1968-69. During the period which the creek flows directly into the ocean, berm sand is added to the shelf area. This pulse of sediment upsets the previous equilibrium and could result in an increase in sand transport.

Second-order ripples were observed within the troughs of primary ripples at 10 of the 27 reference locations (Figs. 22 & 23). The secondary ripples always occurred at depths between 5 and 9 m and were most common in the central and southern portions of the study area. These smaller and shorter-crested ripples usually occurred midway between the crests of the major ripples. It is possible that the smaller ripples form during lower energy conditions that prevailed during the sampling period, and that the larger, primary ripples were the result of earlier, storm-wave conditions. If the primary ripples are formed only during large wave events, then once formed, they would not be easily changed under lower-energy conditions because of their large size. Only another very high-energy wave event would be capable of completely altering these ripples. Because no large storms occurred during this study it is easy to explain why the primary ripple wavelength did not change significantly at any given reference point over time. Further study just before, and immediately after, an intense wave event is necessary to establish proof of this hypothesis.

Another important visual observation involves the variation of grain sizes between ripple troughs and crests (Fig. 24). Previous studies have shown that extremes in grain size occur between ripple troughs and crests (Inman, 1957; Cook and Gorsline, 1972). These studies, which involved ripples in fine- to medium-grain sands, found that the coarsest grains occurred at the ripple crests, and the finest material occurred in ripple troughs. At Monastery Beach the coarsest material was always observed within ripple troughs.

Conclusions

1) Grain sizes and ripple wavelengths decrease with an increase in depth.
2) Large-scale oscillation ripples form under intense wave-generated currents, which are present only during storm conditions. Once formed, lower energy conditions do not change these ripples significantly.
3) Sediment sorting in coarse sands improves with a decrease in depth. Changes in the sorting of sediment in time and space are the result of changes in the wave climate and sediment supply.
4) The head of Carmel Submarine Canyon is locally important in focusing wave energy towards the northern and southern portions of Monastery Beach. This results in spatial variations of grain sizes and ripple wavelengths.
5) Ripple orientations did not change significantly during this study. Primary ripple sets in coarse sands are long-crested and parallel to one another.
6) Gravel to cobble lag deposits occurred in the ripple troughs.

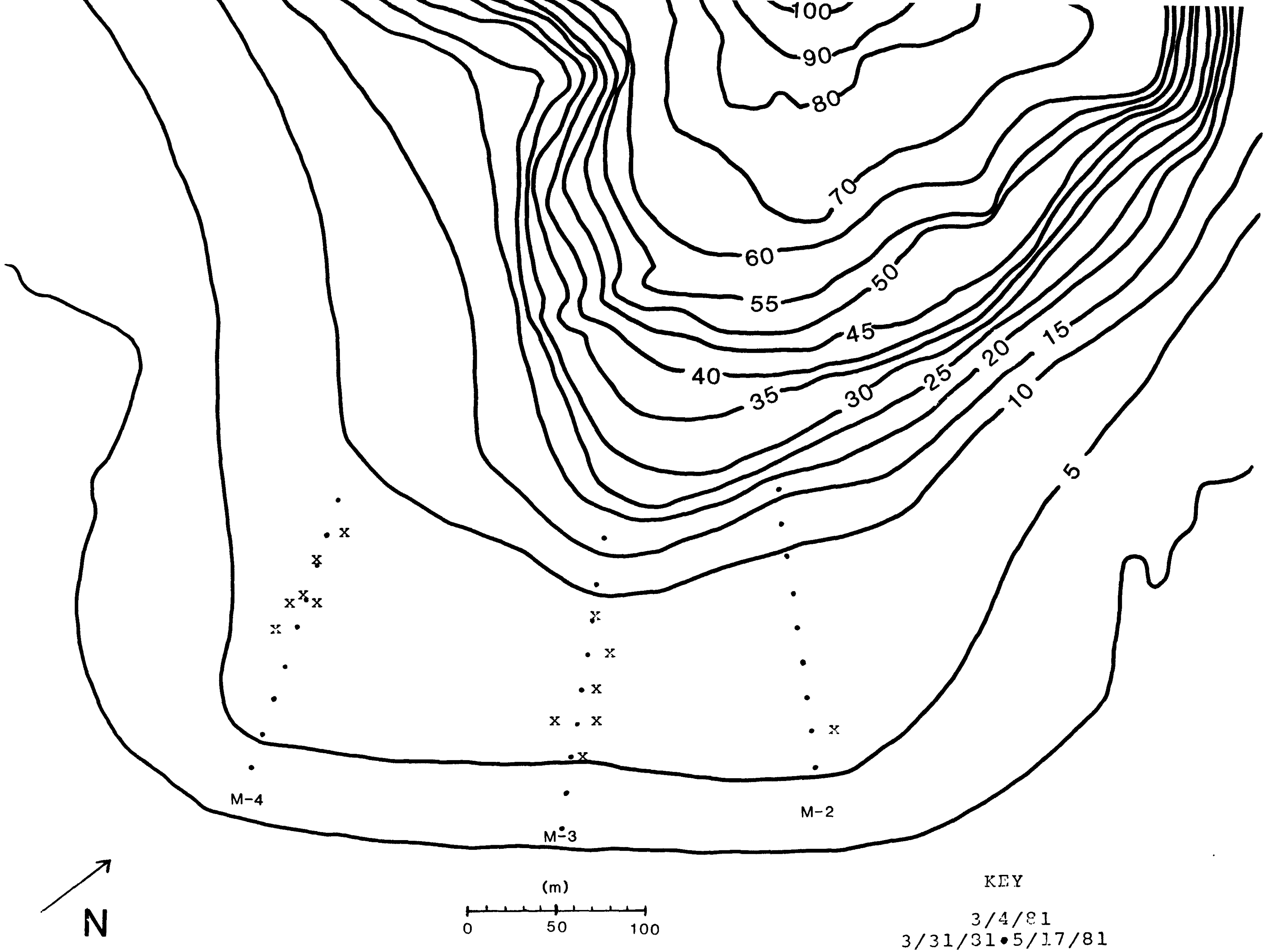

Figure 22. Location of secondary ripple crests. X denotes that at least one secondary ripple was observed to occur at this reference-stake location.

Figure 23.

Diver adjusting T-square for symmetry measure. Note secondary ripple between the primary ripple crests.

Figure 24.

Large-scale oscillation ripples. Note gravel and cobble lag material in trough.

Recommendations for Future Work

1) The maximum ripple wavelength that may occur for a given grain size, needs to be determined so that nearshore reversals in the ripple wavelength can be explained.
2) The contribution of sand to Monastery Beach by the various sources needs to be determined.
3) Wave climate, sand size, and ripple size must be recorded simultaneously. These determine how quickly the ripples respond in very coarse sand, and if the primary large-scale ripples are in equilibrium with the wave climate.
4) Time-lapse photography of the large-scale ripples under differing wave conditions would provide important information on ripple migration, and thus, sand transport.
5) Additional stake height data over the study area is necessary to determine annual changes in sediment deposition and erosion of the shelf area.
6) The reference grid should be expanded to include the head of Carmel Submarine Canyon. Stake height data below the rim of the canyon would provide evidence as to deposition or erosion in this area.
7) More data concerning the occurrence and spacing of secondary ripples should be collected to determine how these ripples form and what influence they have on sediment transport.

Acknowledgments

We wish to thank Bob Anima who provided diving support and valuable technical assistance in constructing field equipment necessary for this study. We also thank Bruce Jaffe and Brent Morinovic who also provided diving assistance.

References

Allen, J.R.L., 1968, "Current Ripples, their relation to patterns of water and sediment motion:" Amsterdam, North-Holland, 433 p.

Bascom, W.H., 1964, "Waves and Beaches:" New York, Doubleday, 267 p.

Clifton, E.H., 1976, Wave formed sedimentary structures - A conceptual model: Society of Economic Paleontologists and Mineralogists, Special Publication No. 24, p. 126-148.

Coastal Data Information Program, (1981): Monthly Reports for March, April, and May. Reports numbers 64, 65, and 66. Sponsored by the U.S. Army Corps of Engineers and the State of California Department of Boating and Waterways.

Cook, D.O., and Gorsline, D.S., 1972, Field observatons of sand transort by shoaling waves: Marine Geology, v. 13, p. 31-55.

Dingler, J.R., and Inman, D.L., 1976, Wave-formed ripples in nearshore sands, from: Proceedings of the 15th Coastal Engineerng Conference, ASCE/Honolulu, Hawaii, p. 2109-2126.

Dingler, J.R., 1981, Stability of a very coarse-grained beach at Carmel, California: Marine Geology, v. 44, p. 241-252.

Folk, R.L., 1974, "Petrology of sedimentary rocks:" Texas, Hemphill, 182 p.

Griffin, P.A., 1969, Heavy mineral investigaton of Carmel Bay beach sands, Master's Thesis, U.S. Naval Postgraduate School, 50 p.

Hirschaut, D.H., 1980, Field observations of osciallatory ripples and sediment parameters in a high-energy nearshore marine environment. Unpublished research paper, University of Santa Cruz, Santa Cruz, California E.S. 143, 31 p.

Inman, D.L., 1952, Measure for describing the size distribution of sediments: Journal of Sedimentary Petrology, v. 22, no. 3, p. 125-145.

Inman, D.L., 1957, Wave-generated ripples in nearshore sands: U.S. Army Corps of Engineers, Beach erosion Board, Technical Memorandum No. 100, 66 p.

Komar, P.D., 1976, "Beach processes and sedimentation:" Englewood Cliffs, New Jersey, Prentice-Hall, 429 p.

Long, A.D., 1973, Ripple formations and their possible causes in the high-energy shallow-water zone at Monestary Bay. Unpublished research paper, California State University of San Jose, Civil Engineering 203, 21 p.

Miller, M.C., and Komar, P.D., 1980, A field investigation of the relationship between osciallatory ripple mark spacing and the nearbottom water orbital motions: Journal of Sedimentary Petrology, v. 50, n. 1, p. 183-191.

Moritz, C.A., Jr., 1968, A descriptive survey of the head of Carmel Submarine Canyon. Masters thesis, U.S. Naval Postraduate School, 79 p.

Miller, R.L., and Zeigler, J.M., 1958, A model relating dynamics and sediment pattern equilibrium in the region of shoaling waves, breaker zone, and foreshore: Journal of Geology, v. 66, p. 417-441.

Miller, R.L., and Zeigler, J.M., 1964, A study of sediment distribution in the zone of shoaling waves of a complicated bottom topography in Papers in Marine Geology, R. L. Miller (ed.): New York, Macmillan, p. 135-153.

National Marine Consultant, 1960, Wave statistics for seven deep water stations along the California coast: U.S. Corps of Engineers, Los Angeles District

National Ocean Survey Tide Tables, 1981, West Coast of North and South America: U.S. Department of Commerce, NOAA, 231 p.

Shepard, R.P., 1973, "Submarine Geology, 3rd edition:" New York, Harper and Row, 517 p.

Wallin, S.R., 1968, The sediments in the head of Carmel Submarine Canyon. Master's thesis, Naval Postgraduate School, 97 p.

Wolf, S.C., 1966, Processes of erosion and sedimentation near the head of Carmel Submarine Canyon, Unpublished research paper, California State University of San Jose, Advanced Physical Geology, 23 p.

Table 1 - Standardized Stake Height Measures

Reference Stake number	Transect M-2 5/17/81	Transect M-2 7/15/81	Net Change	Transect M-4 5/17/81	Transect M-4 7/15/81	Net Change
1	--	--	--	50	35	+15
2	46	40	+6	55	63	-8
3	43	39	+4	--	58	--
4	48	49	-1	73	59	+14
5	39	40	-1	--	54	--
6	--	--	--	50	44	+6
7	37	43	-6	51	47	+4
8	45	19	+16	40	33	+7
9	34	36	-2	45	36	+9

M-2

Average change = +2.2 cm

M-4

Average change = + 6.7 cm

Note: + values indicate deposition

- values indicate erosion

Table 2- Standard Deviation Values (Sorting)

Reference Stake Number		3/4/81 M-3		3/31/81 M-2	3/31/81 M-3	3/31/81 M-4	5/17/81 M-2	5/17/81 M-3	5/17/81 M-4
1	.37	.40		--	.39	.37	.35	.34	
2	.64	.49		.47	.31	.39	.36	.39	
3	.78	.50		.92	.34	.40	.33	.34	
4	.90	.48		.95	.29	.38	.69	.30	
5	.84	.49	1.00	.28	.39	1.07	--		
6	.92	.62	1.10	.28	.39	1.00	.27		
7	.61	.59		.73	.29	.44	.92	.30	
8	--	.81	1.83	.27	.55	--	.32		
9		1.99		1.38	2.15	.31	70	1.89	.30
Average values		.723		.64	.883	.31	.445	.833	.32

Note: The smaller the standard deviation value, the better the degree of sorting.